SPE · AAPG · SEG
CCUS
Carbon Capture, Utilization, and Storage

CCUS: 4430933

Experimental Study of the Geochemical and Mineralogical Changes in the Woodford Caprock Exposed to Carbon Dioxide Saturated Brine

Kojo Acheampong Boateng*[1], Hamid Rahnema [1], William Ampomah[2], Audrey Ayensigna [1], Emmanuel Agyei[1], Godsway Akpabli[1] 1. Petroleum and Natural Gas Engineering, New Mexico Institute of Mining and Technology, Socorro, NM, United States, 2. Petroleum Recovery Research Center, Socorro, NM, United States.

Abstract

Caprock integrity is critical for geological carbon storage (GCS) security. This study investigates the mineralogical and geochemical response of Woodford Caprock Shale, a Silurian-Devonian caprock in the Permian Basin, to CO_2 brine interaction. Ground samples were reacted with synthetic formation brine (TDS=88,643mg/L) under CO_2-rich conditions (138 bar, 138 °C) for three months. Pre and post experimental characterization using X-ray diffraction (XRD), scanning electron microscopy with energy-dispersive spectroscopy (SEM-EDS), and inductively coupled plasma optical emission spectroscopy (ICP-OES) revealed substantial mineralogical reorganization of complete muscovite dissolution (29.1% → 0%), K-feldspar precipitation (31.1% → 47.5%), quartz enrichment (32.3% → 42.9%), dolomite stability (7.4% → 7.6%), and new pyrite formation (2.0%). Brine chemistry showed changes in K^+, Ca^{2+}, and dissolved silica, confirming silicate and carbonate changes. SEM-EDS revealed muscovite dissolution textures and authigenic K-feldspar overgrowths. These findings indicate competing processes as detectable muscovite loss threatens permeability increases, while secondary mineral precipitation may provide self-sealing. Results underscore the need for integrated petrophysical characterization to assess net effects on seal performance.

Introduction

Geological carbon capture and storage (CCUS) is essential for mitigating anthropogenic CO_2 emissions (Hanson et al., 2025). When injecting CO_2 into saline aquifers, it initiates a series of interconnected physical and chemical phenomena (Boison et al., 2024). The long-term integrity of low-permeability caprocks is

critical for preventing upward CO_2 migration (Yeboah et al., 2025). Upon injection, CO_2 dissolves into formation brines, lowering PH and driving mineral dissolution and precipitation reactions that alter porosity, permeability, and sealing capacity (Rathnaweera et al., 2016). The Woodford Shale, a Silurian-Devonian organic-rich mudstone in the Permian Basin, is a primary candidate for CO_2 storage in underlying saline aquifers and depleted reservoirs. Despite its regional importance, experimental studies of its geochemical response to CO_2 -brine systems remain limited. Understanding short-term alteration processes is essential for predicting long-term seal performance and informing site selection and risk assessment. Previous caprock alteration studies have shown variable outcomes, depending on mineralogy and experimental conditions. Phyllosilicate-rich caprocks exhibit higher reactivity than quartz -dominated seals (Zhang et al., 2020). Carbonate dissolution typically dominates early alteration (Rowberry, 2018), while clay mineral transformations control longer-term evolution (Hazen et al., 2013). However, Woodford Shale, characterized by mixed mineralogy including quartz, clays, carbonates, and organic matter, has received limited experimental attention relative to other caprock formations. This study addresses this gap through integrated laboratory experiments combining mineralogical (XRD), microstructural (SEM-EDS), and fluid chemistry (ICP-OES) analyses to quantify short-term mineralogical alteration of Woodford Shale under simulated CO_2 storage conditions (138 bar, 138 °C). Identify dominant reaction pathways controlling mineral dissolution, precipitation, and element redistribution in mixed mineralogy caprocks. Assess implications for seal integrity by linking observed geochemical changes to permeability evolution, buffering capacity, and long-term storage security. By combining pre- and post-reaction characterization with fluid chemistry tracking, this work provides mechanistic insights into caprock-CO_2 interactions essential for site-specific risk assessment and predictive modeling.

Methodology

Woodford Shale caprock samples were collected from 10,611-10614 ft (3,234-3,235 m) depth in the Permian Basin (Silurian-Devonian interval). Samples were dried at 60 °C for 24 hours, mechanically ground, and sieved to < 106-150 μm to increase reactive surface area and accelerate reaction kinetics following established protocols. While powdered samples enhance reaction rates for laboratory timescales, this approach sacrifices intact fabric and may overestimate field-scale alteration rates. Pre-experimental characterization included XRD, SEM-EDS, and thin-section petrography to establish baseline mineralogy and texture.

A synthetic brine representative of Silurian–Devonian Woodford formation water was prepared using analytical-grade salts (NaCl, $CaCl_2 \cdot 2H_2O$, $MgCl_2 \cdot 6H_2O$, KCl, Na_2SO_4) to reproduce a Na–Cl-dominated chemistry with subordinate divalent cations (Table 2A). The brine composition was based on regional formation water data and designed to simulate in situ geochemical conditions. Ground samples (64 g) were loaded into 125 mL stainless steel autoclave reactors with 100 mL synthetic formation brine, representing regional Woodford formation water chemistry (TDS = 88,643 mg/L). The remaining reactor volume was allocated to the CO_2 phase. CO_2 was injected using a Teledyne ISCO 500D syringe pump to 138 bar at 138 °C, simulating storage reservoir conditions. The system was maintained for three months to accelerate geochemical reactions while remaining within laboratory timeframes.

Results

Initial thin-section analysis of the Woodford caprock revealed a finely laminated, organic-rich shale dominated by a clay-rich matrix with dispersed silt-sized quartz. Dolomite occurs as scattered rhombs, while opaque pyrite grains are aligned along laminae, indicating deposition under reducing conditions and preservation of authigenic mineral phases (Figure 1). Semi-quantitative XRD and SEM-EDS analysis revealed substantial mineralogical alterations following 3-month exposure of caprock samples to CO_2-

saturated brine (Na^+, Mg^{2+}, K^+, Cl^-, Ca^{2+}, SO_4^{2-}). (Figure 2a, Figure 3). Detailed brine evolution chemistry is outlined in Figure 2b).

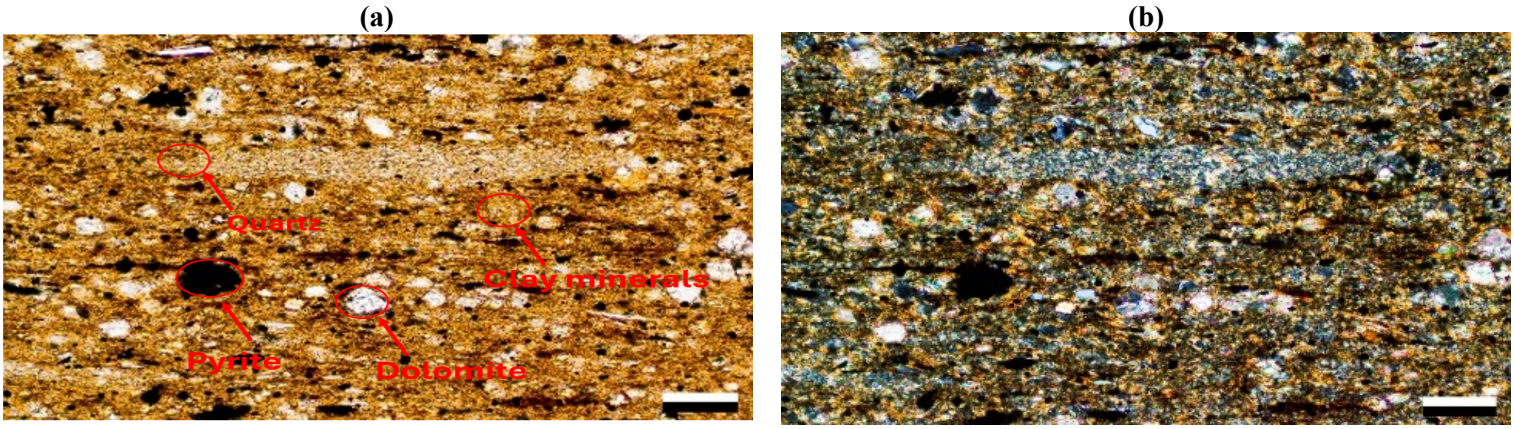

Figure 1: Thin section images of Woodford Caprock under (a) plane-polarized light and (b)cross-polarized light

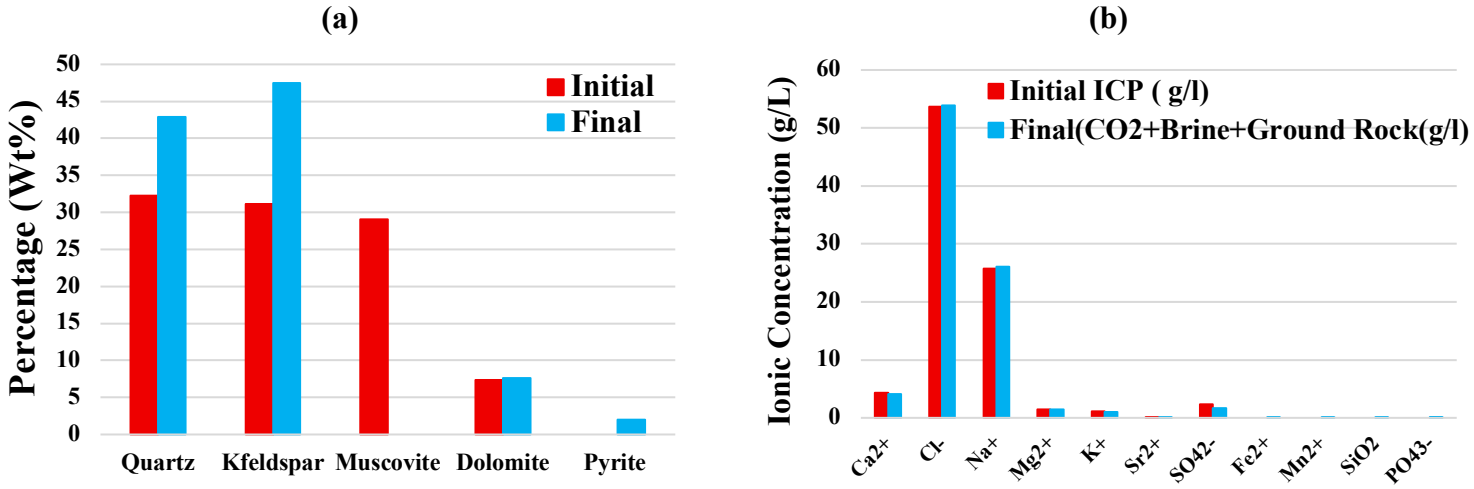

Figure 2: (a) Initial and post-reaction mineralogical composition of the ground rock obtained from X-ray diffraction (XRD) analysis, reported as weight percentage (wt%). (b) Initial and final brine ionic concentrations (g/L) measured by ICP before and after CO_2– brine–ground rock interaction conducted at 138 °C and 138 bar.

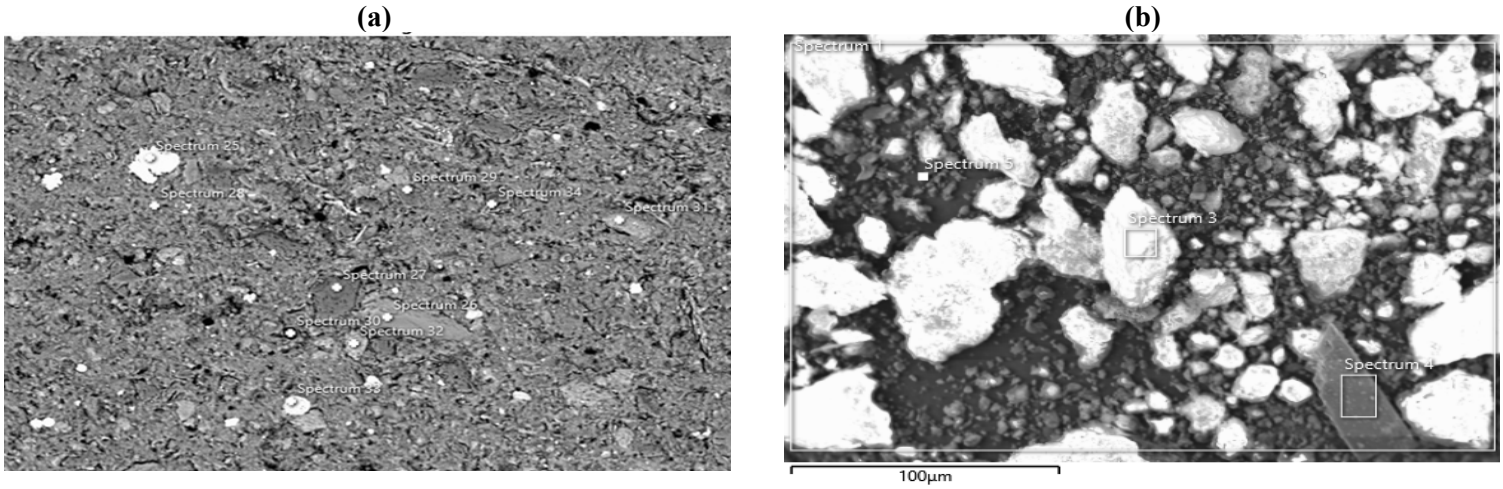

Figure 3: SEM micrographs and corresponding EDS spectra of the rock sample showing (a) initial unreacted surface and (b) post-reaction surface following CO_2–brine exposure.

Discussion

The experimental investigation of CO_2-brine-rock interaction with ground caprock under reservoir conditions (138°C, 138 bar) revealed significant mineralogical and geochemical transformations with critical implications for geological carbon storage. X-ray diffraction analysis demonstrated dramatic mineralogical alterations where there was a complete muscovite dissolution from 29.1% to 0%, substantial quartz enrichment from 32.3% to 42.9%, and K-feldspar increase from 31.1% to 47.5%. This mineral assemblage shift reflects the high susceptibility of phyllosilicate minerals to acid attack in CO_2-enriched environments. The complete breakdown of muscovite released substantial silica, aluminum, and potassium into solution, with partial reprecipitation as framework silicates rather than sheet silicates. The 10.6% relative increase in quartz resulted from silica supersaturation, while the K-feldspar enrichment of 16.4% increase indicated preferential potassium incorporation into secondary feldspar. Additionally, slight dolomite increases from 7.4% to 7.6% and pyrite emergence of 0% to 2%, evidenced by carbonate buffering and localized reducing conditions.

Brine geochemistry evolution provided complementary insights into mineral-fluid interactions. The pH increased from 5.9 to 6.5, demonstrating caprock buffering capacity through carbonate and silicate dissolution, consuming hydrogen ions. Cation dynamics revealed complex patterns as calcium decreased slightly from 4.3 to 4.15 g/L, indicating modest carbonate precipitation; strontium increased dramatically from 0.00271 to 0.00791 g/L a remarkable increase from Sr-bearing phase dissolution; potassium decreased from 1.14 to 1.01 g/L despite muscovite dissolution, confirming incorporation into K-feldspar; and manganese 0 to 0.00295 g/L and iron 0 to 0.0211 g/L appeared via reductive dissolution. Anion transformations included complete sulfate depletion from 2.37g/L to 1.69g/L coupled with pyrite formation, dissolved silica appearance of 0 to 0.0316 g/L reflecting net silicate dissolution, and phosphate emergence of 0.115 g/L. SEM–EDS observations corroborate with XRD post results, showing strong Si–O signals with associated Al and K consistent with quartz enrichment and authigenic K-feldspar formation, while Ca–Mg-rich domains confirm the persistence of carbonate phases. Collectively, these results indicate that CO_2-charged brine promoted selective muscovite dissolution and redistribution of released elements into feldspar and silica phases, rather than extensive bulk mineral dissolution. These findings have profound

implications for CO_2 storage security. The complete clay mineral loss may compromise caprock integrity by reducing plasticity and self-sealing capacity, though quartz cementation could enhance sealing. The pH buffering from 5.9 to 6.5 suggested acid neutralization potential, yet limited carbonate precipitation indicates modest mineral trapping efficiency. Dramatic trace element mobilization, particularly strontium's increase, raises groundwater quality concerns if brine migration occurs, necessitating comprehensive monitoring protocols.

Conclusions

Laboratory experiments simulating CO_2–brine–Woodford Shale interactions under storage-relevant conditions (138 bar, 138 °C, three months) demonstrate substantial mineralogical reorganization driven by coupled fluid–rock reactions. This study demonstrates that phyllosilicate-rich caprocks undergo substantial alteration when exposed to CO_2-rich environments at reservoir conditions. Complete muscovite dissolution, coupled with quartz and K-feldspar enrichment, reveals clay-bearing formation vulnerability to acid-driven transformation. Brine evolution through pH buffering, extreme trace element mobilization and reduction in sulfate. From a CO_2 storage perspective, the demonstrated pH buffering capacity suggests inherent acid mitigation potential, yet limited carbonate precipitation and complete clay mineral loss present challenges for long-term storage security. The clay dissolution could increase permeability through secondary porosity creation, potentially compromising sealing efficiency, though quartz cementation may provide offsetting effects. Critical recommendations include: (1) detailed mineralogical characterization emphasizing clay content in candidate caprocks; (2) coupled geochemical-geomechanical modeling for long-term behavior prediction; (3) monitoring protocols including Sr, Mn, Fe as reaction indicators; (4) site-specific experimental validation; and (5) long-term experiments assessing reaction rate evolution. This research underscores that caprock-CO_2 interactions involve dynamic, multifaceted processes requiring rigorous experimental characterization, sophisticated predictive modeling, and comprehensive monitoring to ensure geological CO_2 storage achieves secure, long-term carbon sequestration while protecting environmental resources.

References

Boison, P. K. N., Ampomah, W., Simmons, J., & Bui, D. (2024). Integrated Geochemical Modeling for CO_2 Sequestration in the San Juan Basin, New Mexico. *SPE Eastern Regional Meeting*, D021S002R002. https://doi.org/10.2118/221374-MS

Hanson, E., Nwakile, C., & Hammed, V. O. (2025). Carbon capture, utilization, and storage (CCUS) technologies: Evaluating the effectiveness of advanced CCUS solutions for reducing CO_2 emissions. *Results in Surfaces and Interfaces*, *18*, 100381. https://doi.org/10.1016/j.rsurfi.2024.100381

Hazen, R. M., Sverjensky, D. A., Azzolini, D., Bish, D. L., Elmore, S. C., Hinnov, L., & Milliken, R. E. (2013). Clay mineral evolution. *American Mineralogist*, *98*(11–12), 2007–2029. https://doi.org/10.2138/am.2013.4425

Rathnaweera, T. D., Ranjith, P. G., & Perera, M. S. A. (2016). Experimental investigation of geochemical and mineralogical effects of CO_2 sequestration on flow characteristics of reservoir rock in deep saline aquifers. *Scientific Reports*, *6*(1), 19362. https://doi.org/10.1038/srep19362

Rowberry, M. (2018). Weathering by dolomite dissolution responsible for the formation of an important paleontological locality in the Prague Synform. *Acta Geodynamica et Geomaterialia*, 297–309. https://doi.org/10.13168/AGG.2018.0022

Yeboah, N. N., Ampomah, W., Bratton, T., Bui, D., & Amosu, A. (2025). Evaluating the Impact of Stress-Induced Changes on Caprock Integrity in the San Juan Basin. *Proceedings of the 2025 Carbon Capture, Utilization, and Storage Conference*. 2025 Carbon Capture, Utilization, and Storage Conference. https://doi.org/10.15530/ccus-2025-4186852

Zhang, F., An, M., Zhang, L., Fang, Y., & Elsworth, D. (2020). Effect of mineralogy on friction-dilation relationships for simulated faults: Implications for permeability evolution in caprock faults. *Geoscience Frontiers*, *11*(2), 439–450. https://doi.org/10.1016/j.gsf.2019.05.014

Appendix

Table A1: Quantitative mineral phase abundances of the Woodford caprock before and after reaction, showing pre-reaction, post-reaction, and absolute percentage changes.

Mineral Phase	Pre Reaction (%)	Post Reaction (%)	Absolute Change (%)
Quartz	32.3	42.9	+10.6
Muscovite	29.1	0	-29.1
K-Feldspar (Total)	31.1	47.5	+ 16.4
*Orthoclase	-	26.9	+26.9
*Sanidine	-	20.6	+20.6
Pyrite	0	2.0	+2.0

Table A2: Major and trace ion concentrations from ICP analysis of brine before and after CO_2–brine–ground rock reaction

ions	**Initial ICP (g/l)**	**Final (CO2 +Brine +Ground Rock) (g/l)**
Ca^{2+}	4.3	4.15
Cl^-	53.7	53.9
Na^+	25.7	26.1
Mg^{2+}	1.42	1.49
K^+	1.15	1.01
Sr^{2+}	0.00271	0.00791
SO_4^{2-}	2.37	1.69
Fe^{2+}	ND	0.0211
Mn^{2+}	ND	0.00295
SiO_2	ND	0.0316
PO_4^{3-}	ND	0.115
TDS	88.64271	86.82856
pH	5.9	6.5

Table A3: Summary of SEM–EDS spectra and corresponding mineral interpretations for the initial Woodford caprock.

Spectrum	**Mineral**
Spectrum 25,33	Pyrite
Spectrum 26	Clay minerals
Spectrum 27	Quartz
Spectrum 28	Muscovite, K Feldspar
Spectrum 29	Dolomite
Spectrum 31 ,32	K Feldspar